Hindawi
International Journal of Energy Research
Volume 2023, Article ID 6056999, 8 pages
https://doi.org/10.1155/2023/6056999

Research Article

Influence of Hydrogen on Vintage Polyethylene Pipes: Slow Crack Growth Performance and Material Properties

Nolene Byrne, Sadeghi Ghanei, Sebastian Manjarres Espinosa, and Michael Neave

Deakin University, Burwood, Victoria, Australia

Correspondence should be addressed to Nolene Byrne; nolene.byrne@deakin.edu.au

Received 27 August 2022; Revised 25 December 2022; Accepted 27 December 2022; Published 4 February 2023

Academic Editor: Pawan Kumar Kulriya

The distribution of hydrogen and how this can be widely achieved plays a significant role in the transition from fossil fuels to clean fuel. Using the existing natural gas pipeline network can be a suitable option for countries with extensive pipeline infrastructure. This study is aimed at investigating the compatibility of the existing polyethylene (PE) distribution pipe network with hydrogen. This paper utilises the cyclic pennsylvania edge notch test (CPENT) method together with material property measurements including melting point, crystallinity, and oxidative induction time (OIT) to understand the impact of exposing two different PE pipe resins to hydrogen at different exposure times. It was found that exposure to hydrogen has a noticeable impact time to failure, while the bulk crystallinity, OIT, and melting point showed little change. A change in crystal orientation was observed, and this likely accounts for the difference in time to failure when exposed to hydrogen.

1. Introduction

The hydrogen economy is expanding as a result of the urgent need to reduce society's dependence on fossil fuels and avoid the harmful consequence of climate change [1–3]. The use of hydrogen to replace natural gas is a promising approach to significantly reduce the carbon emission of the energy sector [2–4]. In order to achieve this, the suitability of the current natural gas pipeline to transport hydrogen is critical [2–4]. Due to the high diffusivity and low density of hydrogen, leakage is a major concern that strongly depends on the pipeline material [4–9]. Some pipeline materials including fibrous cement and cast iron present a higher leakage risk, while polyethylene (PE) pipes have a lower leakage risk [5–8]. PE pipes have been extensively used in the natural gas distribution network for approximately half a century and are potential candidate pipe materials to distribute hydrogen [5–8]. To date, no studies exist investigating the slow crack growth (SCG) performance and linking this to general material properties for PE pipes when exposed to hydrogen.

Failure in PE pipes is characterised by three distinct failure modes that correspond to the circumferential tensile stress experienced by the pipe wall [10–14]. The first failure mode is called ductile failure occurring at high stresses as a result of localised yielding and bulging out at the stress concentration sites [10, 11]. The general mode of failure reported for PE pipes in the field is typically termed quasi-brittle represented by SCG through the pipe wall. This failure mode initiates from a stress-raising defect in the pipe when the circumferential tensile stress is lower than the yield stress of the PE [10–12]. The quasibrittle failure mode is the most common failure mode for in-service PE pipes [10, 13], and PE resin development is aimed at improving the slow crack growth resistance. The final failure mode, brittle failure, occurs after a long period of service time when the circumferential tensile stress is further reduced [10, 11, 14]. In this mode, the stress has a little impact on the service life of the pipe, and the failure initiates due to ageing and polymer degradation [11]. Therefore, understanding the SCG resistance of PE pipes has been extensively used to predict lifetime and degradation of PE pipes [10–14]. Based on the current standard, internal pressure tests for some modern PE pipe grades typically fail after approximately 13 months [13]. In the literature, therefore, there are numerous approaches to measure the SCG performance of PE resins in shorter time frames; all involve an accelerating agent

which may be elevated temperature and/or utilising a preexisting notch in the test samples. Evaluating the SCG behaviour using elevated temperature may face some issues such as the poor or even inverse relationship between the time to failure at elevated and room temperatures [15–17] and presenting macroscopic ductile fracture components which do not necessarily exist at service temperature [18, 19]. Another option to shorten the test time and rank the SCG resistance is to implement a notch in the samples [13] using methods like cracked round bar (CRB) test [20], full notch creep test (FNCT) [21], and Pennsylvania edge notch test (PENT) [22]. Among these various techniques, the CRB test has been successfully used in several studies of the SCG behaviour of PE resins [23–27] using cyclic loading to replace elevated temperature and thus more representative of field-like failure conditions. Despite providing valuable information regarding the service life of various PE pipes, some limitations are associated with the CRB method. The standardised CRB test requires samples with a diameter of more than 10 mm [20] which cannot be met by many of the available PE pipes in the natural gas distribution network [10], which means that the test samples cannot be sectioned directly from the pipe wall and moulding is required which may result in a change of properties or slight degradation during the moulding process. To overcome this limitation, a study [10] developed a new cyclic test at room temperature, called cyclic Pennsylvania edge notch test (CPENT), which investigates notched rectangular samples based on the standardised PENT geometry [22]. The CPENT was able to study samples that were directly sectioned from the PE pipe wall and was successful in distinguishing different PE resins [10].

The paper utilises the CPENT method as well as typical material property measurements including melting point, crystallinity, and oxidative induction time (OIT) to understand the influence of hydrogen on two different PE resin types, a vintage high-density polyethylene (HDPE) pipe and a vintage medium-density polyethylene (MDPE) pipe. Both pipe samples have been utilised in the natural gas network and represent a significant fraction of the existing network both in Australia and worldwide.

2. Materials and Method

2.1. Materials. The studied PE pipes are HDPE class 250 referred to here as PE63 and MDPE PE80B type resin certified to AS/NZS 4130 standard [28], which have previously been in operation within the natural gas network in Australia. PE63 and PE80 types have a minimum required strength of 6.3 MPa and 8 MPa, respectively (expected service life of 50 years at 20°C) [29].

2.2. Hydrogen Gas Exposure Protocol. Samples were exposed to hydrogen gas at room temperature (~25°C) at 80 Bar for various times in a 0.6 litre Parr 4760 series stainless steel pressure vessel equipped with a pressure display module. The system was purged in cycles, 1 barg–40 barg, 1 barg with a nonflammable gas to bring the concentration of oxygen present in the vessel below 0.10% before admitting hydrogen. Subsequently, the system was purged with high purity hydrogen gas following the same cycle protocol until a concentration of ~99.95% hydrogen was achieved.

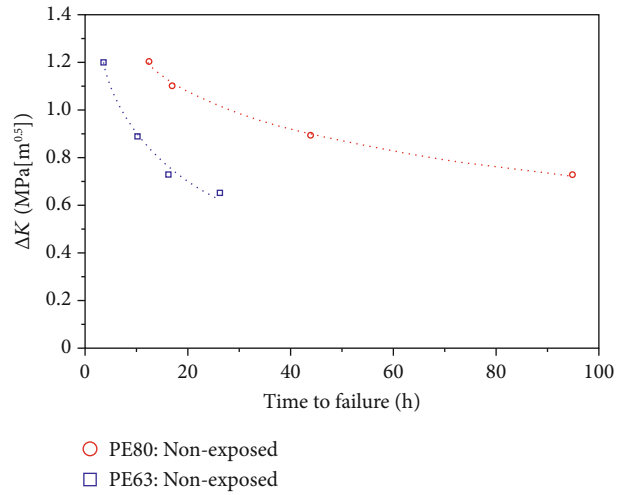

Figure 1: Time to failure as a function of ΔK for PE63 and PE80 pipe samples.

2.3. Cyclic PEN Test (CPENT). The SCG resistance was measured using the cyclic PEN test. This method is described in detail in previous work by the authors [10]. Axial cyclic loading was applied to a rectangular specimen of dimensions 100 mm × 10 mm × 5 *mm* ($l \times w \times t$) with a ~2 mm notch applied by a razor blade. The wall thickness of pipes used in this study was 6.5 mm. Testing was conducted at room temperature using a sinusoidal waveform at an R value of 0.1 and a frequency of 10 Hz.

2.4. Fracture Surface Observation. To study the SCG behaviour of the samples after conducting CPENT, the fracture surface was studied with a low-magnification Olympus SZ61 binocular stereoscopic microscope and a JEOL JSMIT300 scanning electron microscope (SEM). For the SEM studies, the fracture surface was gold coated; then, it was observed at an accelerating voltage of 5 kV.

2.5. Crystallinity Measurement. The % crystallinity of PE (%CPE) samples was evaluated using the Perkin-Elmer DSC 4000 via differential scanning calorimetry (DSC) according to ASTM D3418-15 standard [30]. ~5-6 mg of PE samples was equilibrated at 20°C for 3 minutes before heating to 180°C at a heating rate of 20°C/min. A purge gas of Nitrogen at a 20 mL/min flow rate was used throughout the experiment. The normalized sample enthalpy of fusion melting transition (ΔH_S) was calculated by integrating the area under the fusion endotherm of the DSC curve. The %CPE was determined using Equation (1), where ΔH_f is the enthalpy of fusion of 100% crystalline PE, which is 293 J/g [31]. Triplicates have been taken.

$$\%\text{CPE} = \frac{\Delta H_s}{\Delta H_f} \times 100. \quad (1)$$

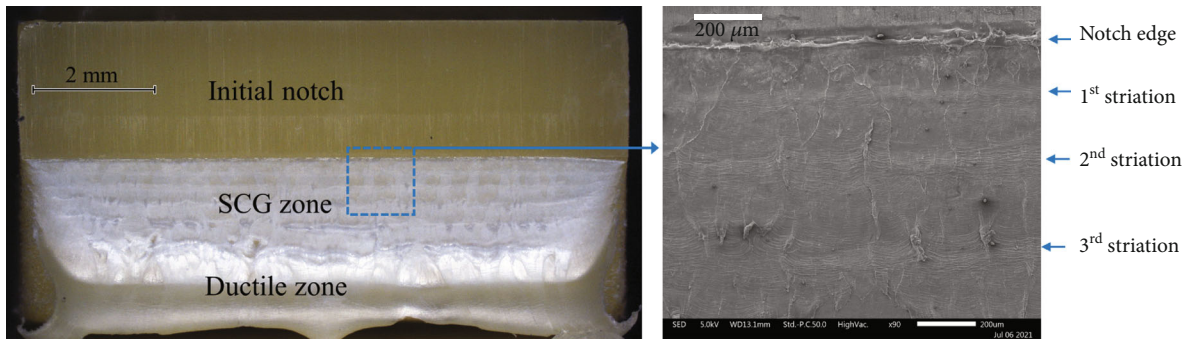

FIGURE 2: The fracture surface of PE80 sample with no exposure to hydrogen tested at $\Delta K = 1.20$ MPa ($m^{0.5}$): (a) indication of different zones using optical microscopy and (b) the indication of the first three striations using SEM observation.

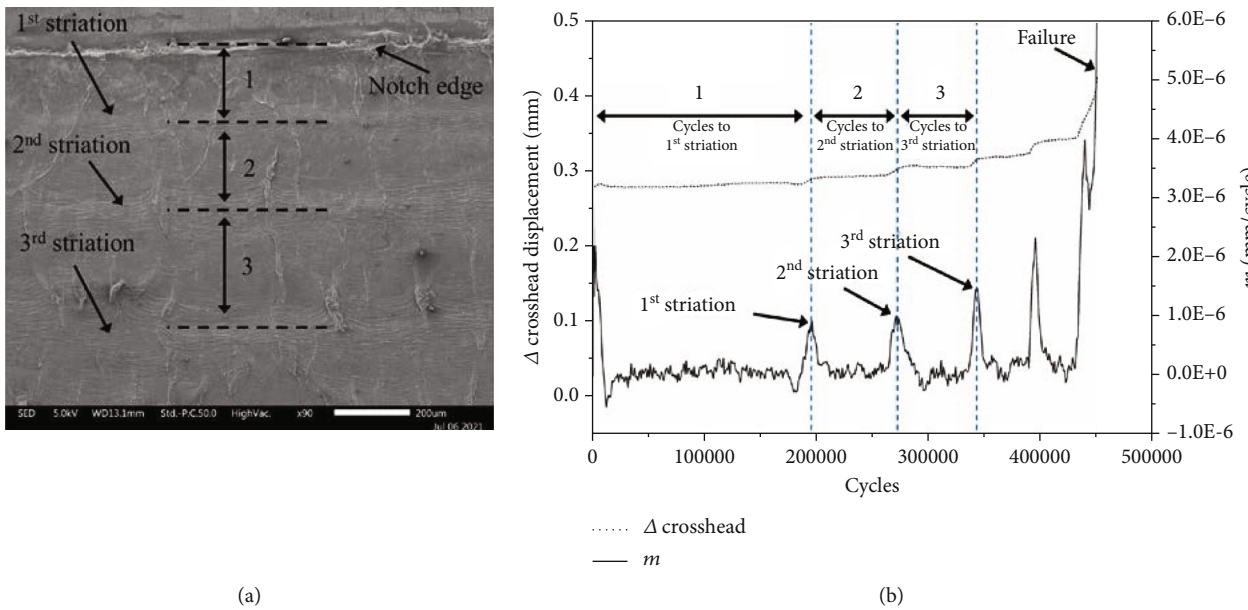

FIGURE 3: An approach to measuring the steady crack growth and detecting striations. (a) Indication of the first three striations on the fracture surface and (b) a comparison between the Δ crosshead vs. cycle and slope vs. cycle curves.

2.6. Oxidative Induction Time (OIT) Measurements. OIT determination using differential scanning calorimetry (DSC) was conducted according to the ASTM D 3895 standard [32]. An isothermal temperature of 210°C was used. Pipe samples (around 4-5 mg) were heated to 210°C in nitrogen flow rate 20 mL/min and held at 210°C for 6 minutes before switching to a compressed air flow of 40 mL/min. Experiments were conducted on the Perkin-Elmer DSC 4000. The onset of the exothermic reaction was taken as the OIT time. Triplicate has been taken.

2.7. Melting Point. The melting point was measured using DSC implementing a scan rate of 10°C/min. The onset is taken as the value for melting point. Triplicates have been taken.

2.8. X-Ray Diffraction. X-ray diffractometry was performed on PE63 before and after 80 bar hydrogen exposure using a Panalytical X-pert Pro MRD texture goniometer on focus mode with a Ni-filtered Cu Kα radiation source at 40 kV acceleration voltage and 30 mA current over the 2θ range from 10^0 to 70^0 at a rate of 0.01^0 every 3 seconds. Triplicate measurements performed.

3. Results and Discussion

3.1. Fatigue Resistance of Vintage HDPE and MDPE Pipes. Figure 1 compares the time to failure for the two vintage PE pipe resin types at different stress concentration factor (ΔK) [10] values. It can be seen from Figure 1 that at all ΔK MPa ($m^{0.5}$) values, the time to failure for PE80 is longer than that for PE63. PE63 is a high density PE type, while PE80 is a medium density PE. PE80 was developed with the aim at improving the slow crack growth resistance. This is confirmed in Figure 1 and is an expected result [10].

3.2. Identifying Stable Crack Growth. Figure 2(a) shows the fracture surface of the PE80 sample with no exposure to

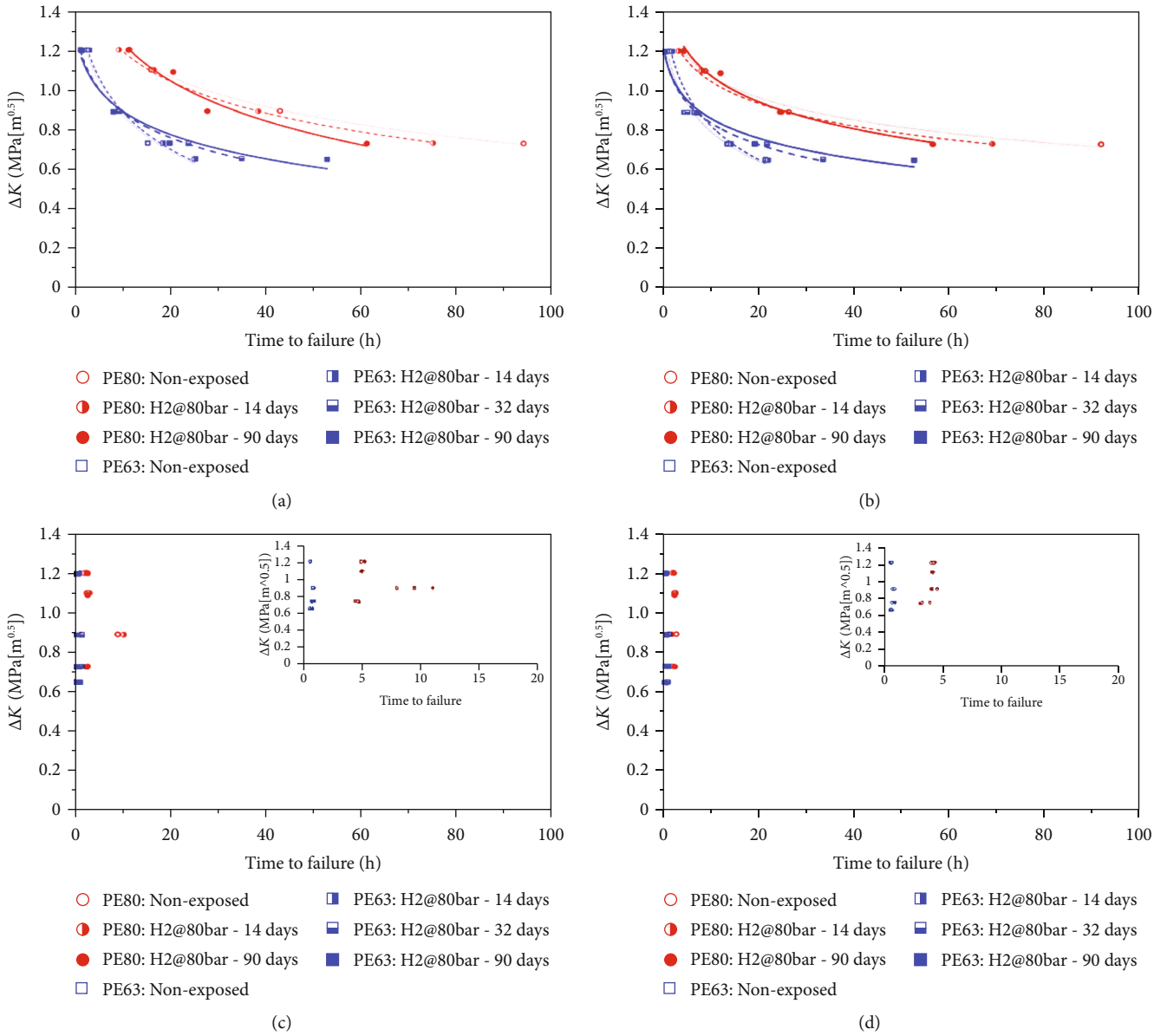

FIGURE 4: (a) Time to failure, (b) time to 1st striation initiation, (c) time to 2nd striation initiation, and (d) time to 3rd striation initiation as a function of ΔK MPa ($m^{0.5}$) for PE63 and PE80 pipe samples that were differently exposed to hydrogen.

hydrogen in which the CPENT was carried out at ΔK = 1.20 MPa ($m^{0.5}$). Below the notch area, the fatigue striation marks can be observed even at a low magnification, which is followed by a distinctive ductile failure region (Figure 2(a)). These fatigue striations are true crack arrest markings on the fracture surface of polymers [33]. As can be observed in Figure 2(b), for each striation, the damage accumulation continues in the craze zone until reaching a point where the next cycle of loading results in jumping the crack tip to the craze boundary and forms a striation; then, this process repeats, and the formation of the next striation starts.

Considering a stepwise SCG behaviour, the cyclic stress builds up ahead of the crack tip and accumulates the damage, until a point where the crack jumps forward, arrests then releases the accumulated stress, and leaves a striation mark on the fracture surface (Figure 3(a)). The stepwise SCG behaviour at a micromechanics level can be attributed to the crack opening in the longitudinal direction that is obtained from the fatigue test equipment. Based on the PENT test methodology, the SCG rate can be approximately considered the same as the rate of crack opening displacement for a given condition [15]. Figure 3(b) illustrates an example of this correlation, showing Δ crosshead displacement = maximum crosshead displacement − minimum crosshead displacement values as a function of the loading cycles. Neglecting the first jump at the beginning of the test which is due to adjusting the equipment's grips with the CPENT sample; the plot of Δ crosshead displacement versus cycles shows a plateau for almost the first 200 K cycles. Then, the first step in the curve marks the point of the 1st striation occurrence, and the following steps can be related to the occurrence of the next striation and so on until a sharp jump in the curve is visible which is due to the final

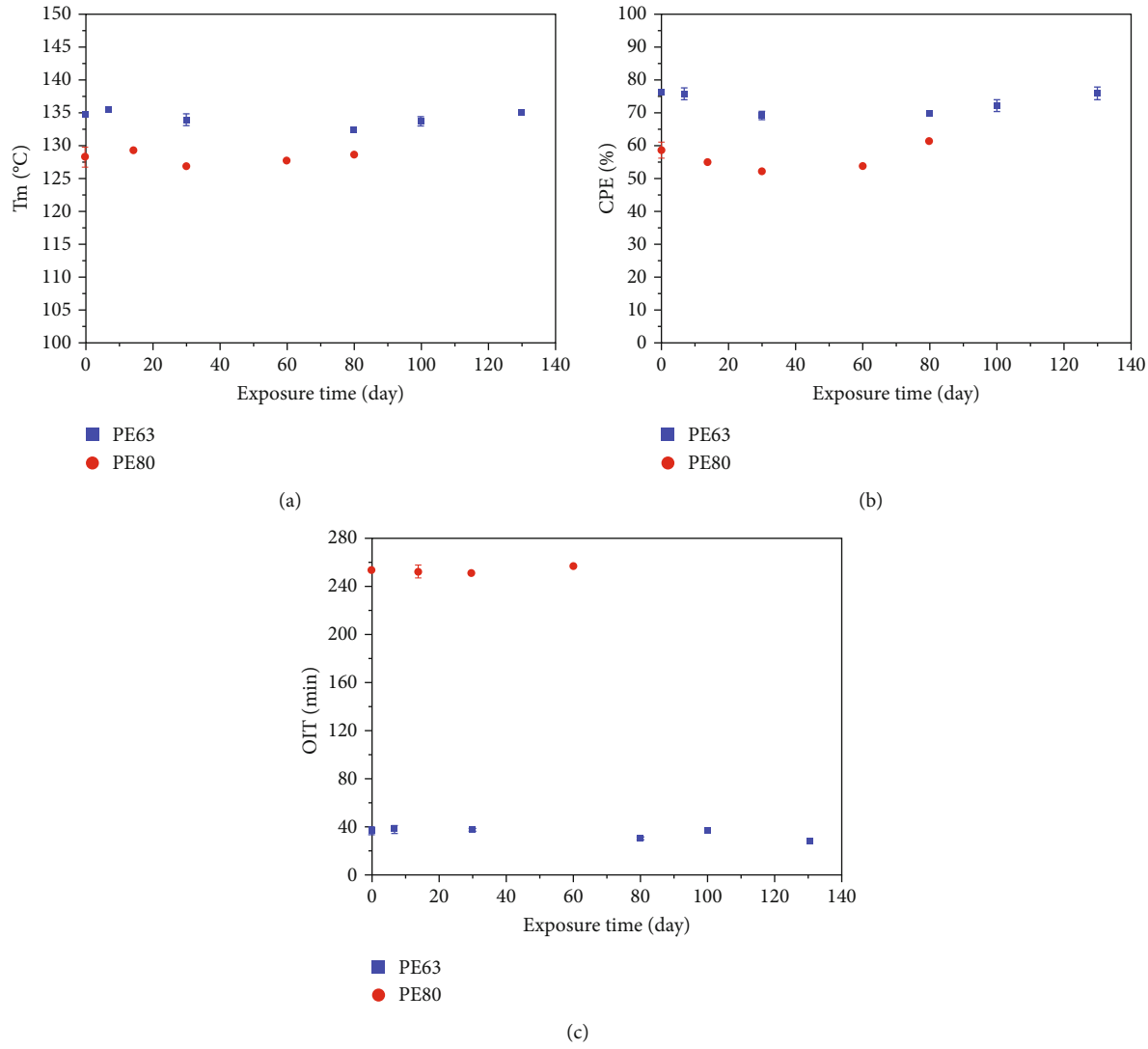

Figure 5: PE63 and PE80 pipe samples that were differently exposed to hydrogen for different time intervals. (a) melting point (T_m), (b) crystallinity (CPE), and (c) oxygen induction time (OIT).

ductile failure. To identify the occurrence of the striations which is linked to the steps in the Δ crosshead displacement versus cycle curve, the slope of the curve (m) was calculated using the following equation:

$$m = \frac{\text{Displacement}_2 - \text{Displacement}_1}{\text{Cycle}_2 - \text{Cycle}_1}. \quad (2)$$

When the damage is building up ahead of the crack tip in the craze zone, the slope of the displacement curve does not significantly change. After jumping the crack to the craze boundary and forming a visible striation mark, a significant change in the slope of the displacement curve can be observed (Figure 3(b)). Therefore, a point where a significant peak can be observed in the slope curve can be attributed to the cycle that resulted in the formation of a striation mark. Subsequently, the time taken to reach each striation can be determined. As indicated in Figure 3(b), the time to the 1st striation initiation starts from the first cycle and ends when the 1st significant change in the slope is observed. The time to the 2nd striation starts from the cycle that is linked with the 1st striation mark and ends when the 2nd striation mark is formed. The time to the other striations can be similarly measured.

As shown in Figure 3(b), the ratio of the number of cycles to initiate the 1st striation to the final failure is the largest when compared with the other striations. Thus, the 1st striation plays a significant part in the total time to failure for the PE pipe. In literature, the ratio of crack initiation or 1st striation initiation to the time to final failure varies from 0.2 to 0.6 and strongly depends on the resin type [15, 34].

3.3. The Impact of Hydrogen on Slow Crack Growth Behaviour. Figure 4(a) shows the time to failure as a function of ΔK for PE63 and PE80 at various hydrogen exposure times. For the PE80 pipe, the exposure to the hydrogen has almost no impact on the time to failure at higher ΔK values of 1.09 MPa ($m^{0.5}$) and 1.20 MPa ($m^{0.5}$) across all exposure

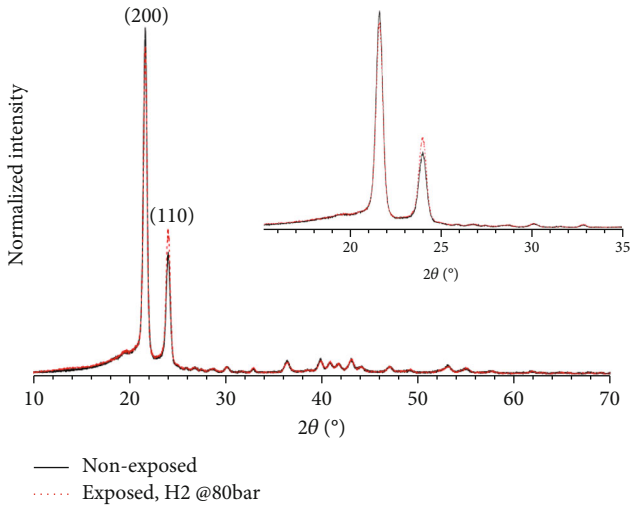

Figure 6: The X-ray diffractograms of the APA36 (PE63) sample from previous report where black is the nonexposed and red is the 180 days exposed condition.

times. However, at lower ΔKs, 0.89 MPa ($m^{0.5}$) and 0.73 MPa ($m^{0.5}$), the time to failure of the PE80 was reduced by 35% and 22%, respectively. A similar trend is seen for the PE63 pipe, whereby at the higher ΔK values, 0.89 MPa ($m^{0.5}$) and 1.20 MPa ($m^{0.5}$), respectively, the time to the failure remains almost the same for the unexposed and unexposed samples. However, as the ΔK is lowered, the time to failure for the PE63 exposed samples is increased, suggesting an improvement in the fatigue resistance. The time to the failure of the PE63 sample that was tested at $\Delta K = 0.65$ MPa ($m^{0.5}$) is almost doubled when exposed to hydrogen for 90 days. In other studies, the long time of exposure to hydrogen resulted in no deleterious effect on the mechanical properties of the studied PE pipes [6], or even slightly improved them [7, 8]. The results in Figure 4(a) indicate that the exposure to hydrogen does not change the time to failure of the PE63 and PE80 samples tested at larger ΔKs, which suggest that the stress has a more significant impact on the failure rather than exposure to hydrogen. On the other hand, for samples tested at lower ΔKs, the exposure to hydrogen is the governing factor in determining the time to failure. As such, the results presented here indicate that the influence of hydrogen will likely depend greatly on the type of PE resin being exposed as well as the expsoure conditions, including pressure and time. As previously discussed in Section 3.2, the time to the 1st striation for the nonexposed sample was a significant portion of the total time to failure. It can be seen, in Figure 4(b), that when the samples are exposed to hydrogen again, the time to the 1st striation is the dominant portion of the total time to failure; this is true for both PE resin types and for all ΔKs investigated here.

As the crack progresses, as shown by the fracture surface (Figure 3(a)), higher order striations form. Here, the time needed to initiate the 2nd and 3rd striations are shown in Figures 4(c) and 4(d), respectively. Interestingly, the time to the 2nd and 3rd stration is very short relative to the time to the 1st stration, and neither the applied cyclic stress or the hydrogen exposure time seems to have an impact on the time to the 2nd and 3rd striations, see Supplementary table 1. Therefore, it can be suggested that under these conditions, the progress of the crack through the sample does not appear to be significantly influenced by the applied stress or hydrogen exposure time with the time to the 1st striation being the major contributor to the total time to failure.

3.4. Material Properties. While the SCG and failure behaviour of PE pipes is a critical factor in determining pipe service lifetimes, other material properties such as the melting point, crystallinity, and OIT also can impact pipe service life [10]. Figure 5 shows the various material properties as a function of hydrogen exposure for both the PE63 and PE80 resins. It can be seen that the melting point for both PE63 and PE80 is very similar and shows no significant change with hydrogen gas exposure; the crystallinity for PE80 is measured to be lower than that for PE63; this is expected as PE80 is a medium density polyethylene; again, hydrogen exposure shows no significant change in the crystallinity of either PE resin pipe. Finally, Figure 5(c) shows the oxygen induction time for both the PE63 and PE80; here, PE63 has a lower OIT value than PE80 which represents the fact that PE63 has been in service for longer than PE80; again, however, hydrogen gas has no significant impact on the OIT for either PE63 or PE80.

While the total crystalline component of the polymers showed no significant change when exposed to hydrogen, the orientation of the crystals does appear to have undergone a shift. The XRD pattern for the PE63 sample exposed to hydrogen for 45 days and unexposed sample is shown in Figure 6. The characteristic (110) and (200) crystal planes can be seen in both diffractograms. However, for the hydrogen exposed condition (dotted red), a decrease in intensity of the (110) plane coupled with an intensity increase of the (200) plane is measured. This suggest that a shift in the crystal orientation has occurred causing one crystal plane to become more "in focus" of the incident beam, while the other one is shifting away from the beam focus. This slight rotation in the crystal orientation after hydrogen exposure may contribute to the difference in failure behaviour observed between the exposed and unexposed samples.

4. Conclusion

The use of the natural gas network for the distribution of hydrogen will enable the replacement of natural gas with hydrogen. Here, the impact of hydrogen gas on polyethylene pipe resins, PE63, and PE80 has been investigated. Both these resins are considered to be vintage and currently existing in the network. It was found that hydrogen exposure had no significant impact on the material properties, melting point, crystallinity, and OIT for both PE63 and PE80. The SCG resistance was also measured as a function of hydrogen exposure at different exposure times. For the PE63 and PE80 samples tested at larger ΔKs, the time to failure was not affected by the exposure to hydrogen; however, the exposure to hydrogen did seem to influence the time to failure for

samples tested at lower ΔKs. The time to the failure of the PE63 sample that was tested at the lowest ΔK of 0.65 MPa ($m^{0.5}$) was almost doubled when exposed to hydrogen for 90 days when compared to the nonexposed pipe. On the other hand, the time to the failure for the PE80 sample tested at the lowest ΔK of 0.73 MPa ($m^{0.5}$) was decreased by 22% when exposed to hydrogen for 90 days. Here, it was shown that the time to the 1st striation was a significant component of the total time to failure, while the time to 2nd and 3rd striations was very short and was not changed by the value of the applied stress of hydrogen, indicating that hydrogen may impact crack initiation.

Data Availability

The data is available by request to corresponding author.

Conflicts of Interest

The authors declare that they have no conflicts of interest.

Acknowledgments

This work is funded by the Future Fuels CRC, supported through the Australian Government's Cooperative Research Centres Program. We gratefully acknowledge the cash and in-kind support from all our research, government, and industry participants. Open access publishing facilitated by Deakin University, as part of the Wiley - Deakin University agreement via the Council of Australian University Librarians.

Supplementary Materials

Supplementary Table 1 shows the time to each stration for 0 and 90 days, H_2 expsoure for each resin type. *(Supplementary Materials)*

References

[1] S. Hosseini, "Hydrogen has found its way to become the fuel of the future," *Future Energy*, vol. 1, no. 3, pp. 11-12, 2022.

[2] A. M. Oliveira, R. R. Beswick, and Y. Yan, "A green hydrogen economy for a renewable energy society," *Current Opinion in Chemical Engineering*, vol. 33, article 100701, 2021.

[3] A. Ahmed, A. Q. al-Amin, A. F. Ambrose, and R. Saidur, "Hydrogen fuel and transport system: a sustainable and environmental future," *International Journal of Hydrogen Energy*, vol. 41, no. 3, pp. 1369–1380, 2016.

[4] R. B. Gupta, *Hydrogen Fuel: Production, Transport, and Storage*, CRC Press, 2008.

[5] I. A. Gondal and M. H. Sahir, "Prospects of natural gas pipeline infrastructure in hydrogen transportation," *International Journal of Energy Research*, vol. 36, no. 15, pp. 1338–1345, 2012.

[6] M. H. Klopffer, P. Berne, S. Castagnet, M. Weber, G. Hochstetter, and E. Espuche, "Polymer Pipes for Distributing Mixtures of Hydrogen and Natural Gas: Evolution of Their Transport and Mechanical Properties after an Ageing under an Hydrogen Environment," in *18th World Hydrogen Energy Conference 2010 - WHEC 2010*, Essen, Germany, 2010.

[7] R. R. Ratnakar, N. Gupta, K. Zhang et al., "Hydrogen supply chain and challenges in large-scale LH2 storage and transportation," *International Journal of Hydrogen Energy*, vol. 46, no. 47, pp. 24149–24168, 2021.

[8] H. Iskov and S. Kneck, "Using the natural gas network for transporting hydrogen – ten years of experience," in *International Gas Union Research Conference*, Rio de Janeiro, 2017.

[9] W. J. Jasionowski, J. B. Pangborn, and D. G. Johnson, "Gas distribution equipment in hydrogen service," *International Journal of Hydrogen Energy*, vol. 5, no. 3, pp. 323–336, 1980.

[10] R. De Silva, T. Hilditch, and N. Byrne, "Assessing the integrity of _in service_ polyethylene pipes," *Polymer Testing*, vol. 67, pp. 228–233, 2018.

[11] Y. Liu, Y. Li, X. Liu, W. Luo, B. Yang, and M. Li, "A time dependent process zone model for slow crack growth of polyethylene pipe material," *Journal of Physics: Conference Series*, vol. 1634, no. 1, article 012140, 2020.

[12] Y.-f. Qian, F.-p. Yang, H.-f. He, and H.-y. Du, "Experimental study on the fatigue crack growth and overload effect in medium density polyethylene," *Journal of Materials Engineering and Performance*, vol. 29, no. 10, pp. 6681–6690, 2020.

[13] A. Frank, F. J. Arbeiter, I. J. Berger, P. Hutař, L. Náhlík, and G. Pinter, "Fracture mechanics lifetime prediction of polyethylene pipes," *Journal of Pipeline Systems Engineering and Practice*, vol. 10, no. 1, article 04018030, 2019.

[14] K. Q. Nguyen, C. Mwiseneza, K. Mohamed, P. Cousin, M. Robert, and B. Benmokrane, "Long-term testing methods for HDPE pipe - advantages and disadvantages: a review," *Engineering Fracture Mechanics*, vol. 246, article 107629, 2021.

[15] E. Nezbedová, P. Hutař, M. Zouhar, Z. Knésl, J. Sadílek, and L. Náhlík, "The applicability of the Pennsylvania notch test for a new generation of PE pipe grades," *Polymer Testing*, vol. 32, no. 1, pp. 106–114, 2013.

[16] G. Pinter, W. Balika, and R. W. Lang, "A correlation of creep and fatigue crack growth in high density poly(ethylene) at various temperatures," in *European Structural Integrity Society*, L. Rémy and J. Petit, Eds., pp. 267–275, Elsevier, 2002.

[17] A. Frank, G. Pinter, M. Kapur, and E. Nezbedová, "Comparison of accelerated tests for PE grades lifetime assessment," *Proceedings of Plastic Pipes*, vol. 16, no. 24, 2012.

[18] R. K. Krishnaswamy, A. M. Sukhadia, and M. J. Lamborn, "Is PENT a True Indicator of PE Pipe Slow Crack Growth Resistance? Bulletin, Performance Pipe," Report No. PP818-TN, Plano, TX, 2007, http://www.hdpe.ca/wp-content/uploads/2016/03/PP818-TN-PENT-Slow-Crack-Growth-Resistance.pdf.

[19] N. Brown and J. M. Crate, "Analysis of a failure in a polyethylene gas pipe caused by squeeze off resulting in an explosion," *Journal of Failure Analysis and Prevention*, vol. 12, no. 1, pp. 30–36, 2012.

[20] *ISO 18489: Polyethylene (PE) Materials for Piping Systems — Determination of Resistance to Slow Crack Growth under Cyclic Loading — Cracked Round Bar Test Method*, International Organization for Standardization ISO Central Secretariat Chemin de Blandonnet, Geneva, Switzerland, 2015.

[21] Standardization, I.O.f., *ISO 16770: Plastics — determination of environmental stress cracking (ESC) of polyethylene — full-notch creep test (FNCT)*, International Organization for Standardization ISO Central Secretariat Chemin de Blandonnet, Geneva, Switzerland, 2019.

[22] *ISO 16241: Notch Tensile Test to Measure the Resistance to Slow Crack Growth of Polyethylene Materials for Pipe and*

Fitting Products (PENT), International Organization for Standardization ISO Central Secretariat Chemin de Blandonnet, Geneva, Switzerland, 2005.

[23] B. Gerets, M. Wenzel, K. Engelsing, and M. Bastian, "Slow crack growth of polyethylene—accelerated and alternative test methods," in *Deformation and Fracture Behaviour of Polymer Materials*, W. Grellmann and B. Langer, Eds., pp. 177–187, Springer International Publishing, Cham, 2017.

[24] A. Frank, G. Pinter, and R. W. Lang, "Prediction of the remaining lifetime of polyethylene pipes after up to 30 years in use," *Polymer Testing*, vol. 28, no. 7, pp. 737–745, 2009.

[25] G. Pinter, M. Haager, W. Balika, and R. W. Lang, "Cyclic crack growth tests with CRB specimens for the evaluation of the long- term performance of PE pipe grades," *Polymer Testing*, vol. 26, no. 2, pp. 180–188, 2007.

[26] M. Haager, G. Pinter, and R. Lang, "Ranking of PE-HD pipe grades by fatigue crack growth performance," *Plastics Pipes*, vol. XIII, p. 11, 2006.

[27] A. Frank and G. Pinter, "Evaluation of the applicability of the cracked round bar test as standardized PE-pipe ranking tool," *Polymer Testing*, vol. 33, pp. 161–171, 2014.

[28] *AS/NZS 4130:2018 - Polyethylene (PE) pipes for pressure applications*, American National Standards Institute, NY, United States, 2018.

[29] *ISO 4427-1: Plastics Piping Systems for Water Supply and for Drainage and Sewerage under Pressure — Polyethylene (PE) — Part 1: General*, International Organization for Standardization ISO Central Secretariat Chemin de Blandonnet, Geneva, Switzerland, 2019.

[30] International, A, *ASTM D3418: Standard Test Method for Transition Temperatures and Enthalpies of Fusion and Crystallization of Polymers by Differential Scanning Calorimetry*, American National Standards Institute, NY, United States, 2021.

[31] A. J. Hadi, G. J. Hadi, K. B. Yusoh, G. F. Najmuldeen, and S. F. Hasany, "Prediction of experimental measurement data for high density polyethylene and polypropylene solubility in organic solvents," *Chemical Product and Process Modeling*, vol. 12, no. 3, 2017.

[32] International A, *ASTM D3895-19: Standard Test Method for Oxidative-Induction Time of Polyolefins by Differential Scanning Calorimetry*, American National Standards Institute, NY, United States, 2019.

[33] M. D. Hayes, D. B. Edwards, and A. R. Shah, "4 - Fractography basics," in *Fractography in Failure Analysis of Polymers*, M. D. Hayes, D. B. Edwards, and A. R. Shah, Eds., pp. 48–92, William Andrew Publishing, Oxford, 2015.

[34] X. Lu and N. Brown, "A test for slow crack growth failure in polyethylene under a constant load," *Polymer Testing*, vol. 11, no. 4, pp. 309–319, 1992.